Catalytic Grafting: A New Technique for Polymer–Fiber Composites. III. Polyethylene–Plasma-treated Kevlar™ Fibers Composites: Analysis of the Fiber Surface

QI WANG,[1] SERGE KALIAGUINE,[2] and ABDELLATIF AIT-KADI[1,*]

[1]CERSIM and [2]CERPIC, Department of Chemical Engineering, Laval University, Quebec, Quebec, G1K 7P4, Canada

SYNOPSIS

In this article, plasma-treated Kevlar™ fiber–polyethylene composites prepared by the catalytic grafting technique were studied. The reactive groups —COOH, —OH, —NH₂ generated on the Kevlar fiber surface by oxygen plasma treatment were used to chemically anchor Ziegler–Natta catalyst, which was then followed by ethylene polymerization on the fiber surface. The surface structure of the Kevlar fibers, untreated or treated by oxygen plasma, catalyst grafted, or ethylene polymerized, was characterized by X-ray photoelectron spectroscopy (XPS), attenuated total reflection (ATR), and scanning electron microscopy (SEM). The morphology, interfacial behavior, and mechanical properties of the high-density polyethylene (HDPE) composites reinforced by either catalytic grafted or ungrafted Kevlar fibers were investigated by means of differential scanning calorimetry (DSC), polarized light optical microscopy, tensile testing, and SEM. Special attention was devoted to the tensile properties of the composites in the direction transverse to the fibers. The experimental results show that oxygen plasma treatment increases the reactive site concentration on the fiber surface significantly and that the composites reinforced by catalytically grafted Kevlar fibers exhibit higher tensile strength both parallel and transverse to the fibers. The improved interfacial adhesion is attributed to the interfacial chemical bonding established by catalytic grafting. © 1993 John Wiley & Sons, Inc.

INTRODUCTION

Fiber-reinforced polymers play an important role in our modern society. The main objectives in designing a new composite material are, first, to obtain a material with tailored properties and, second, to find a reinforcing material (generally in the form of fibers) and a polymer matrix whose mixture will have improved properties not attainable by the constituents of the composite separately. However, poor adhesion between the polymer matrix and the reinforcing fibers still remains a problem for getting polymer composites with high performance. Great efforts have been devoted to improving the interfacial behavior of polymer composites. The optimum choice to improve interface adhesion would be to establish

chemical bonds across the interface.[1] In previous papers,[2,3] we presented a new technique for preparing polymer–fiber composites, designated as catalytic grafting. This technique is based on the chemical anchoring of a catalyst on reinforcing agents containing reactive groups on their surface and then conducting an olefin polymerization on the supported catalyst. The fibers with chemically anchored catalyst will act as a supported catalyst for olefin polymerization and a reinforcing agent for the final product. The chemical bonds established between the matrix and the fibers improve the adhesion while the polymer grafted on the active sites of each fiber ensures a good dispersion and wetting of the fibers in the synthesized matrix, resulting in a significant improvement of mechanical properties. Asbestos-polyethylene composites obtained in this way exhibit much better properties than those of the composites made by *in situ* polymerization or conventional mixing.[2] Moreover, solvent extraction performed on

---

the same composites using decalin for 20 h showed that less than 43% of polyethylene could be extracted from the catalytic grafted composite while all the polyethylene was extracted from the other composites under the same conditions.[2] This technique was also extended to ultrahigh-modulus PE (UHMPE) fiber–high-density polyethylene HDPE system when the fibers were treated by oxygen plasma and reactive groups were generated on the fiber surface. The polyethylene grafted on the fibers acted as a transition layer between the reinforcing UHMPE fibers and a commercial HDPE matrix, improving the interfacial adhesion quite significantly.[3] The main limitation with this type of reinforcement is its relatively low melting point restricting the number of thermoplastics that can be used as matrices. The technique was also used to obtain composites with high fiber content, which could be used as an effective modifier for the conventional polymer–fiber composites.[4]

Among the synthetic fibers used as reinforcing material for polymer composites, Kevlar™, a fiber made from poly(para-phenylene terephthalamide) and commercialized by DuPont, has attracted great attention because it combines excellent mechanical properties and thermal stability as well as low density. It has been widely used in the aeronautical industry in the form of epoxy composites. But as far as thermoplastic composites are concerned, the application of Kevlar fibers is limited, mainly due to the poor adhesion of these fibers with most thermoplastic resins.[5] Various treatments have been attempted to enhance the adhesion of Kevlar with thermoplastics: roughening the fiber by water treatment,[6] bromination,[7] metalation,[8] and chemical grafting by reaction of NH_2 end groups at the fiber surfaces with methacryloyl chloride[9] or suberoyl chloride.[10] However, some authors[11] have analyzed the chemical composition of the Kevlar fiber surface and reported that there are very few —NH_2 groups lying at the Kevlar fiber surface. Hydrolysis[12] and cold plasma treatment have been employed to increase the concentration of the reactive chemical groups on the Kevlar fiber surface. Plasma treatment is of special interest, because it involves only a surface modification, the bulk properties of the fibers, which are crucial for reinforcing materials, being preserved.

In this study we applied the catalytic grafting technique to the oxygen plasma-treated Kevlar fiber–HDPE system. The reactive sites on Kevlar fibers greatly enhanced by oxygen plasma treatment were used to chemically anchor a Ziegler–Natta catalyst. This was then followed by ethylene polymer-

ization on the fiber surface. X-ray photoelectron spectroscopy (XPS), attenuated total reflection (ATR), and scanning electron microscopy (SEM) were employed to characterize the surface structure of the Kevlar fibers before and after oxygen plasma treatment, catalyst grafting, and ethylene polymerization. Differential scanning calorimetry (DSC), polarized light optical microscopy, tensile testing, and SEM were used to investigate the morphology, interfacial behavior, and mechanical properties of the HDPE composites reinforced by catalytic grafted or ungrafted Kevlar fibers. Special attention was focused on the properties in the direction transverse to the fibers.

EXPERIMENTAL

Materials

The polyethylene used in this study was a HDPE XS84672.07 from Dow Chemical (melt flow index of 6.0 g/10 min). Kevlar fibers made from poly(p-phenylene terephthalamide) by DuPont were treated by Plasma Science using a cold oxygen plasma at room temperature for 1 min. $TiCl_4$ and $Al(C_2H_5)_3$ were used as catalyst and cocatalyst for ethylene polymerization. The ethylene (Canadian Liquid Air) used as monomer was dried and deoxygenated by bubbling through hexane containing a small amount of $Al(C_2H_5)_3$ before polymerization. Hexane was also used as solvent during polymerization after it was dried with sodium for 1 day and distilled under nitrogen.

Preparation of Composites

The procedure for catalyst anchoring and the following Ziegler–Natta polymerization of ethylene on the fiber surface were described elsewhere.[2] The difference with the present system is that the Kevlar fiber being a long fiber, a monofilament of a given length was wound on a plastic frame. Several such frames were fitted together at a distance of 2 mm from each other and introduced in the reactor. A magnetic stirring bar was used during the catalyst grafting reaction as well as during ethylene polymerization.

Two different plasma-treated Kevlar fiber–HDPE composites, namely, a composite reinforced by the catalytically grafted Kevlar fiber (KEG) and a composite reinforced by the ungrafted Kevlar fiber (KEF), were prepared. The fibers were wound parallel to each other on HDPE frames and then sand-

wiched between previously pressed HDPE films, pressed at 160°C for 10 min using a 6-ton Carver laboratory press. The sample was cooled to 120°C, held for 10 min, and then cooled to room temperature under press. The dumbbell specimens for tensile testing were cut in the directions parallel or transverse to the fibers from these compressed sheets.

Composite films each containing a single filament of either the catalytic grafted or ungrafted Kevlar fiber were prepared in a similar way for examination under the optical microscope.

Characterization

The surface morphologies of the four kinds of Kevlar fibers, namely, before (KOR) or after (KPL) oxygen plasma treatment, reacted with catalyst (KTI) and covered with the catalytic grafted polyethylene (KPOLY), as well as the HDPE composites reinforced by grafted (KEG) and ungrafted (KEF) Kevlar fibers were examined through a Jeol JSM-III SEM microscope. The surface structure of the four kinds of fibers was analyzed by XPS and ATR. X-ray photoelectron spectroscopy measurements were carried out using a V.G. Scientific Escalab Mark II spectrometer with a hemispherical analyzer operated in the constant-pass-energy mode (20 eV except N_{1s}, for which the pass energy was 15 eV). A Mg Kα X-ray source ($h\nu$ = 1253.6 eV) operated at 15 kV was used. The residual gas pressure in the spectrometer chamber during data acquisition was below 10^{-8} torr. The C_{1s} binding energy value of hydrocarbons (285.0 eV) was used as an internal reference. The experimental intensities of XPS peaks were determined using linear background subtraction and integration of peak areas.[13] When required, XPS peaks were deconvoluted using routine procedures.[13] The ATR infrared measurement of the fiber surface was conducted using a Bomem DA3.02 spectrophotometer with 2 cm^{-1} resolution. ZnSe was used as the reflection element. The spectra were obtained by 1000 scans and smoothed using the Spectra-Cal software. The melting endotherms of KPOLY, KEF, and KEG samples were determined using a computerized Perkin-Elmer DSC-4 at a heating rate of 10°C/min. The composite films containing a single filament were observed through a Zeiss optical microscope fitted with a Mettler FP-80 temperature-regulated hot stage between 120 and 135°C at a heating rate of 1°C/min. Photographs were taken at given temperatures. The mechanical properties of the two different composites were examined using an Instron tensile instrument at a crosshead speed of 0.5 cm/min.

RESULTS AND DISCUSSION

Kevlar fibers (registered trademark of E.I. DuPont de Nemours Co.) are generally considered to be composed of poly(*para*-phenylene terephthalamide) (PPTA),[11] the chemical formula of which can be written as
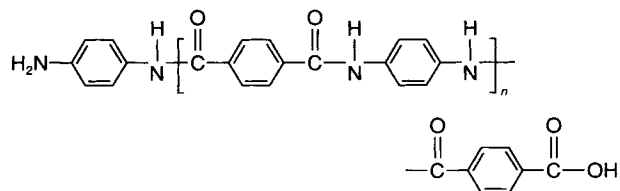
Scheme 1

The concentration of reactive chemical groups is limited due to the chemical structure of the macromolecules. However, the essential step involved in the catalytic grafting technique is anchoring a Ziegler–Natta catalyst on the fiber surface, which requires many reactive chemical groups, —COOH, —OH, —NH$_2$, etc., on the fiber surface. The cold-gas oxygen plasma treatment used here can effectively modify the surface structure of the Kevlar fibers at no expense of their bulk properties. It is well established[14] that the radicals, electrons, ions, and photons present in the oxygen plasma collide with the polymer, breaking covalent bonds and creating free radicals on the polymer surface. The polymer free radicals react with other species in the plasma environment to introduce functional chemical groups. In our case, the —COOH, —OH, and —NH$_2$ groups generated on the Kevlar fiber surface were used to anchor TiCl$_4$. The reaction may be described as follows[9,15]:
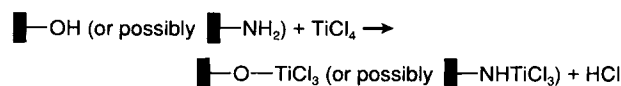
Scheme 2

The Kevlar fibers with chemically anchored TiCl$_4$ served as a supported catalyst for ethylene polymerization. As soon as Al(C$_2$H$_5$)$_3$, the cocatalyst, was injected into the reactor under positive pressure of ethylene, the fibers became brownish at once, and ethylene polymerized on the fiber surface. After 30 min, the polymerization was terminated by adding ethanol. Scanning electron microscopy allowed us to observe the morphology changes happening on the Kevlar fiber surfaces after they were subjected to oxygen plasma treatment, Ziegler–Natta catalyst anchoring, and ethylene polymerization. It can be seen from Figure 1 that little change in surface mor-
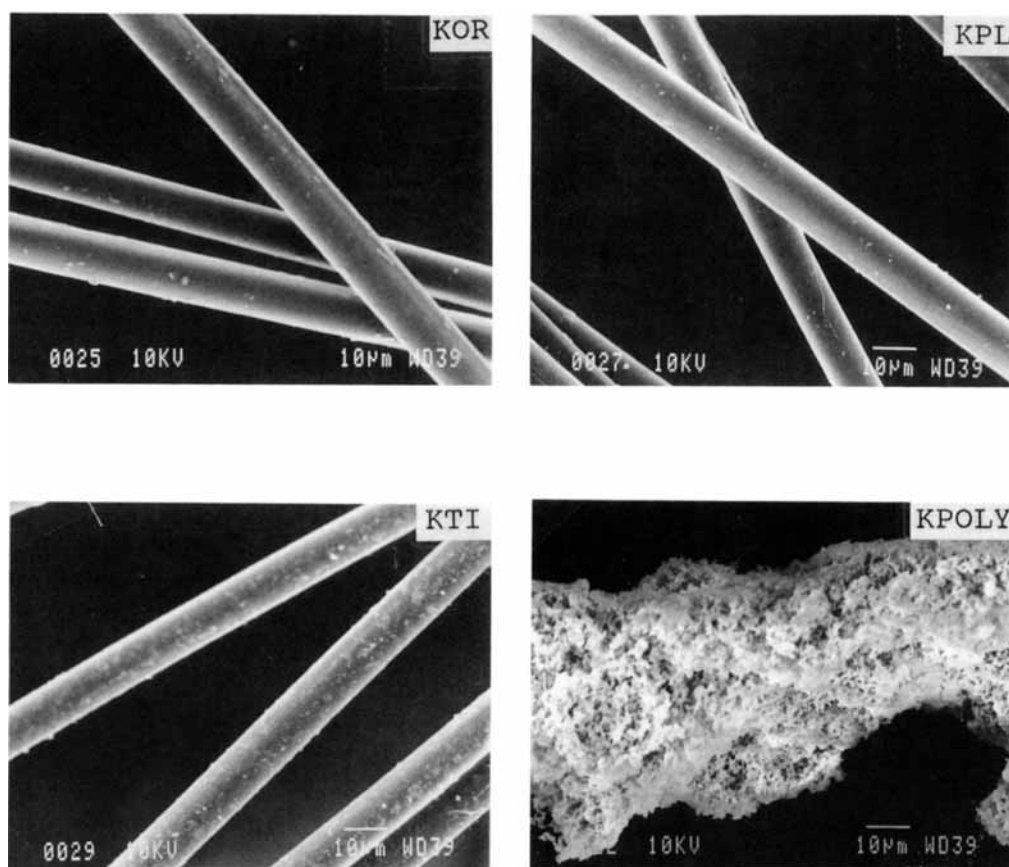
Figure 1   Scanning electron micrographs of original (KOR), plasma-treated (KPL), catalyst-grafted (KTI), and polymerized (KPOLY) Kevlar fibers. (×1000)

phology takes place after plasma treatment (compare the original Kevlar fiber, KOR, with the plasma-treated Kevlar fiber, KPL), while the catalyst grafting acts as a chemical etching, roughening the fiber surface (compare KPL with the catalyst-grafted Kevlar fiber, KTI). It is obvious that the catalytic grafted polyethylene covers the fiber, forming a polymer coating on its surface (see the ethylene-polymerized Kevlar fiber, KPOLY).

X-ray photoelectron spectroscopy allows to analyze the chemical changes occurring on Kevlar fibers during these procedures. Table I gives a general survey of the surface atomic distribution of the elements of interest for the four samples based on the routine calculation of the peak area of XPS lines. The parameters listed in Table I are:

A_m: the measured photoelectron intensity for one XPS line.

A_n: the normalized peak area, calculated according to the following equation:

$$A_n = \frac{A_m \, \Delta E}{n \, \Delta t} \qquad (1)$$

where ΔE is step size, Δt is time per channel, and n is the number of scans.

σ: Scofield cross section corrected for angular effects.

X_a: the relative atomic concentration, calculated based on the following equation:

$$X_a \approx \frac{A_n(a)/\sigma(a)}{\sum\limits_{i=1}^{n} A_n(i)/\sigma(i)} \qquad (2)$$

For the untreated Kevlar fiber (as received, KOR), according to the structure formula, there are 2 oxygen atoms, 2 nitrogen atoms, and 14 carbon atoms per one repeat unit of Kevlar, that is, the ratio O/C and the ratio N/C should be 1/7 (0.143). It can be seen from Table I that N/C is 0.125, is roughly coincident with the calculated value in the error range, and O/C is 0.189, which is little higher than the theoretical value. This is reasonable due to the possible surface oxidation during fiber fabrication[12] and the simplifications involved in Eq. (2). After
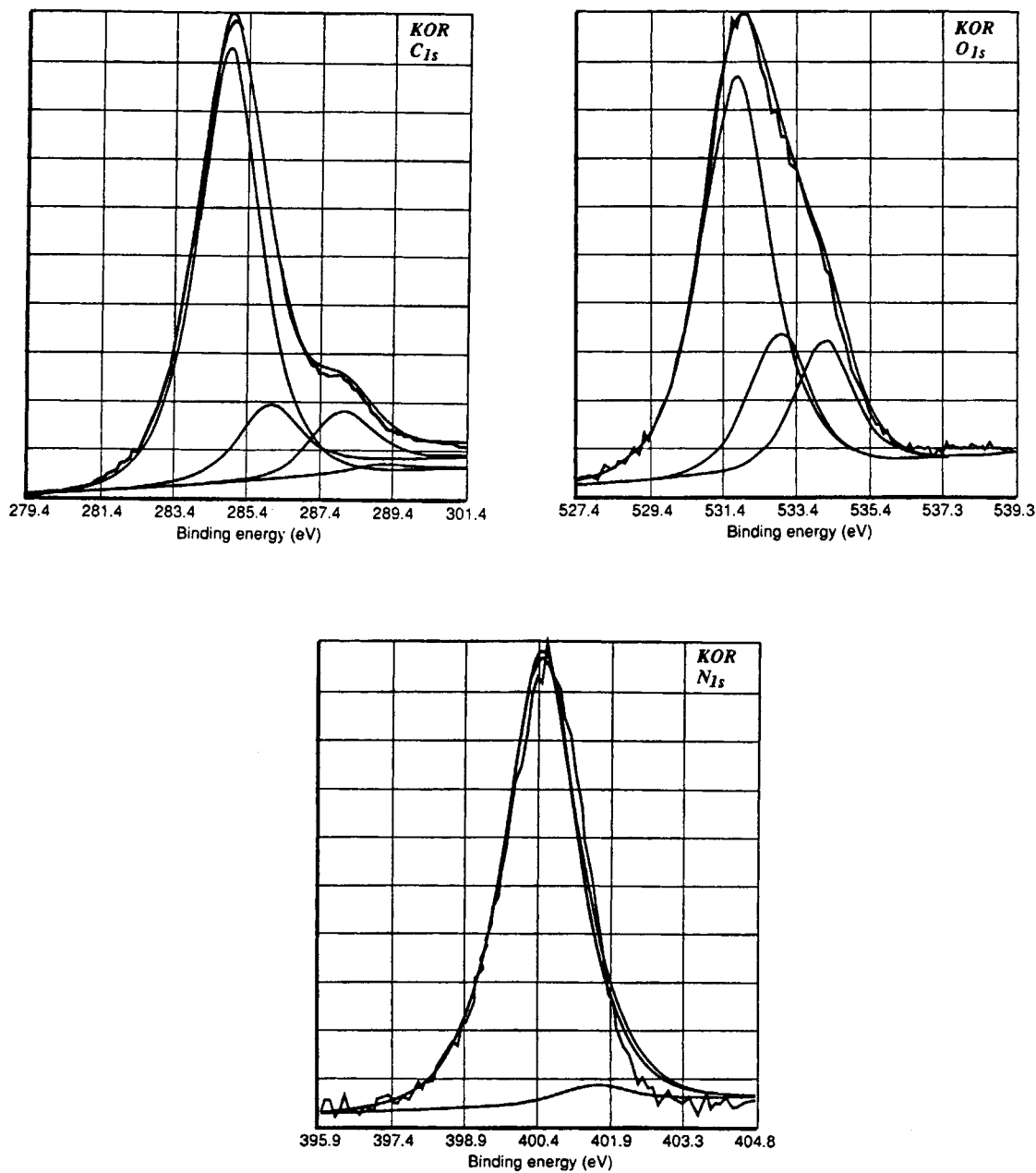
Table I   Surface Composition of KOR, KPL, KTI, and KPOLY Determined by XPS

Sample	Element	A_m	A_n/σ	X_a, %	Atomic Ratio
KOR	C_{1s}	1,067,532	0.287	76.1	O/C, 0.189; N/C, 0.125
	O_{1s}	501,699	0.054	14.4	
	N_{1s}	133,492	0.036	9.5	
KPL	C_{1s}	947,216	0.354	73.1	O/C, 0.272; N/C, 0.096
	O_{1s}	667,221	0.096	19.9	
	N_{1s}	155,688	0.034	7.0	
KTI	C_{1s}	791,240	0.196	56.5	O/C, 0.562; N/C, 0.063;
	O_{1s}	811,888	0.110	31.8	Cl/Ti, 0521
	N_{1s}	87,786	0.012	3.5	
	Cl_{2p}	74,071	0.009	2.7	
	Ti_{2p}	649,286	0.019	5.2	
KPOLY	C_{1s}	628,742	0.311	73.3	O/C, 0.216; Cl/Ti, 2.840
	O_{1s}	387,162	0.067	15.8	
	N_{1s}	—	—	—	
	Cl_{2p}	140,871	0.013	3.2	
	Ti_{2p}	195,276	0.005	1.1	
	Al_{2p}	34,924	0.028	6.6	

oxygen plasma treatment (KPL), the O/C ratio increased to 0.272, indicating an effective modification of the fiber surface. For the fibers modified by reacting with $TiCl_4$ (KTI), the O/C ratio is very high, up to 0.562, and the Cl/Ti ratio is too low, only 0.521, compared to the theoretical value 3.0 (see Scheme 2). This is probably due to the fact that part of the oxygen atoms comes from the oxidation of the anchored catalyst when the fibers are exposed to air. This phenomenon will be discussed later in this work. After catalytic grafting polymerization of ethylene on the fiber surface (KPOLY), it is interesting to note that the intensity of nitrogen becomes almost zero, no signal being detected above the noise. This is the consequence of polymer coating, because the thickness of polyethylene grafted on the fibers is beyond the analysis depth of XPS. For the same reason, the oxygen of the Kevlar fibers should not be detected. The 0.216 value observed for the O/C ratio in KPOLY would therefore be in part due to adventitious TiO_2 formed during titanium grafting by reaction of $TiCl_4$ with traces of humidity that may still have been present in the hexane. These particles would not be strongly linked to the fiber and would therefore not be covered by the polyethylene film. This would explain why Ti is detected in the XPS spectrum of the KPOLY sample. The examination of Figure 1 indeed shows some microcrystals on the KTI fibers not detected on KPL. These are most likely TiO_2 particles. In addition, the oxygen detected in sample KPOLY may in part be due to the termination of the polymerization by

ethanol, which deactivates the catalysts and also introduces oxygen atoms into this sample. The Cl/Ti ratio of this sample is 2.88. According to the previous discussion, the fact that this value is close to the theoretical 3.0 value of $—O—TiCl_3$ would be fortuitous. The increased Cl/Ti ratio compared to KTI is however interesting. The fraction of Ti atoms that bear Cl ligands at the surface of the KTI sample, namely, the sites active in polymerization, are indeed imbedded in polyethylene on KPOLY and therefore not detected by XPS. The fact that chlorine is visible by XPS is in line with the accepted view that this ligand stays as the end group of the polyethylene chain.[16] Thus chlorine remains present at the external surface of the polyethylene film.

More information about the four samples could be obtained by deconvolution of C_{1s}, O_{1s}, and N_{1s} peaks. Figure 2 shows the C_{1s}, O_{1s}, and N_{1s} spectra of the original Kevlar fiber, KOR. X-ray photoelectron spectroscopy allows distinction of four kinds of carbon atoms as indicated in Scheme 3 and Table II:

Scheme 3

Figure 2 C_{1s}, O_{1s}, and N_{1s} spectra of KOR.

where C_1 stands for the carbon atoms of the —C—C—C— structure from the benzene ring, C_2 for the carbon atoms of the —C—C—N— structure, C_3 for the carbon atoms in the amide group —CONH—, and C_4 for the carbon atoms of —COOH, which may have resulted either from the end groups of the macromolecules or the surface oxidation due to the manufacturing process. Also, there are four kinds of oxygen atoms, as indicated in Scheme 4:
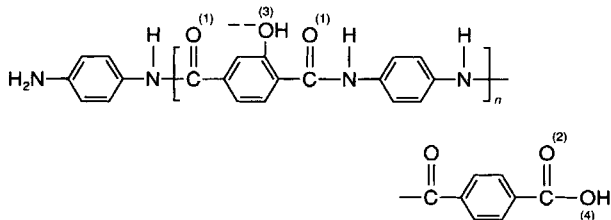
Scheme 4

where O_1 stands for the oxygen atoms in the amide

Table II   Results of Peak Deconvolution of C_{1s}, O_{1s}, and N_{1s} Spectra of KOR

Atom No.	From Structure	BE_{ref}, eV	BE_{exp}, eV	$(P_j/\Sigma\ P_i)_{exp}$	$(P_j/\Sigma\ P_i)_{theor}$
C_1	—C—C̲—C—	285.0[17]	285.0	0.677	0.714
C_2	—C—C̲—N—, —C—O—	286.3[17]	286.1	0.142	0.143
C_3	—CONH—	287.8[17]	288.1	0.132	0.143
C_4	—COOH	289.0[17]	289.0	0.049	~ 0
O_1	—CONH—	531.6[18]	531.8	0.592	$1 - 2x$[a]
O_2	O̲=C—OH	532.8[18]	533.0	0.209	x
O_3	—C—OH	533.7[18]	—	—	0
O_4	O=C—O̲H	534.3[18]	534.2	0.199	x
N_1	—CONH—	401–402[19]	400.5	0.922	$1 - x$
N_2	$PhNH_2$	401–402[19]	401.5	0.078	x

[a] $x = 1/n = 1/(DP - 2)$ if the chain was entirely visible by XPS; DP is degree of polymerization.

group —CONH—; O_2 for the double-bonded oxygen atoms in the acid group O=C—OH; O_3 for the oxygen atoms in the hydroxyl group —C—OH, which are generated by oxygen plasma treatment; and O_4 for the single-bonded oxygen in the acid group O=C—OH. The N_{1s} peak can also be deconvoluted into two lines, N_1 stands for the nitrogen atoms in the amide group —CONH— and N_2 stands for the nitrogen atoms in the amine group —NH_2. Table II lists the results of deconvolution of C_{1s}, O_{1s}, and N_{1s} spectra for the KOR sample. Assuming a complete absence of C–OH in the Kevlar polymer, an estimate of the N–C ratio can be calculated as $C_2/(C_1 + C_2 + C_3 + C_4)$. The calculated value of 0.142 is in good agreement with the 0.143 value calculated from Scheme 1. This is also in rather good agreement with the measured N/C value of 0.125 (Table I). Similarly, the O/C atomic ratio may be estimated as $(C_3 + 2C_4)/(C_1 + C_2 + C_3 + C_4)$. The deconvolution of the C_{1s} confirms that

there exists a small amount of —COOH, the C_4 fraction being equal to 0.049. This conclusion can also be drawn from the deconvolution of the O_{1s} peak. The contents of the double-bonded oxygen, O_2, and the single-bonded oxygen, O_4, are 0.209 and 0.199, respectively. They should be equal to each other if they originate from carboxylic groups. The difference is of the order of experimental errors in peak-area deconvolution. Also, the ratio O_2/O_1 (0.353) is comparable with the ratio C_4/C_3 (0.371). According to Scheme 1, the fraction of NH_2 groups should be very small and equal to $1/n$. From the 7.8% fraction of N_2, a value of $n \approx 14$ is calculated, which is certainly below the bulk n value. It is therefore concluded that the end groups —NH_2 and —COOH are more exposed to the fiber surface than the other groups in the chain.

Figure 3 shows the C_{1s}, O_{1s}, and N_{1s} spectra of the plasma-treated Kevlar fiber (KPL), and Table III lists the results of deconvolution of C_{1s}, O_{1s}, and

Table III   Results of Peak Deconvolution of C_{1s}, O_{1s}, and N_{1s} Spectra of KPL

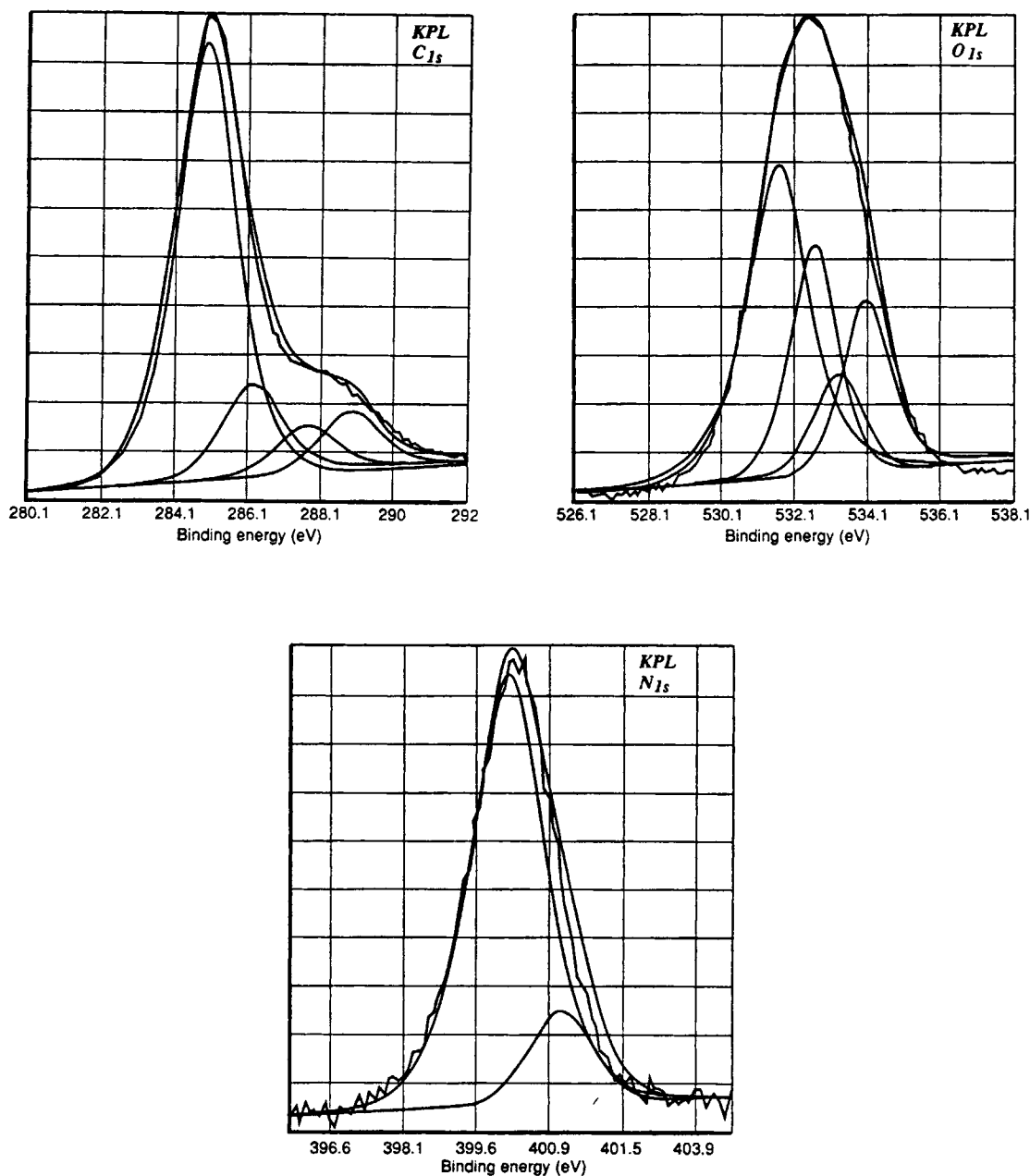| Atom No.	From Structure	BE_{ref}, eV	BE_{exp}, eV	$P_j/\Sigma\ P_i$
C_1	—C—C̲—C—	285.0	285.0	0.616
C_2	—C—C̲—N—, —C—O—	286.3	286.3	0.158
C_3	—CONH—	287.8	287.8	0.103
C_4	—COOH	289.0	289.0	0.123
O_1	—CONH—	531.6	531.7	0.418
O_2	O̲=C—OH	532.8	532.7	0.254
O_3	—C—OH	533.7	533.4	0.127
O_4	O=C—O̲H	534.3	534.1	0.202
N_1	—CONH—	401–402	400.3	0.808
N_2	$PhNH_2$	402–403	401.4	0.192

Figure 3 C_{1s}, O_{1s}, and N_{1s} spectra of KPL.

N_{1s} peaks. The most significant differences between the spectra of plasma-treated (KPL) and original fibers (KOR) are the increase in C_4 and N_2 and the appearance of an O_3 component. These changes suggest that the plasma treatment involves both the hydrolysis of the CN bond in the amide group creating —NH_2 and —COOH functional groups and the hydroxylation of the benzene ring creating —C—OH groups. These changes would be responsible for the increase in O/C reported in Table I.

Figure 4 shows the C_{1s}, O_{1s}, and N_{1s} spectra of the Kevlar fiber reacted with $TiCl_4$ (KTI), and Table IV lists the deconvolution results of C_{1s}, O_{1s}, and N_{1s} peaks. After anchoring $TiCl_4$ on Kevlar fibers, Ti replaces one hydrogen atom of —COOH or —C—OH (or maybe —NH_2), resulting in the formation of species with the structure of —$COOTiCl_3$ or $COTiCl_3$ (or maybe $NHTiCl_3$). For C_{1s} deconvolution, the binding energies for C_2 and C_3 for sample KTI were the same as those for sample KPL, because Ti is not directly linked to a carbon
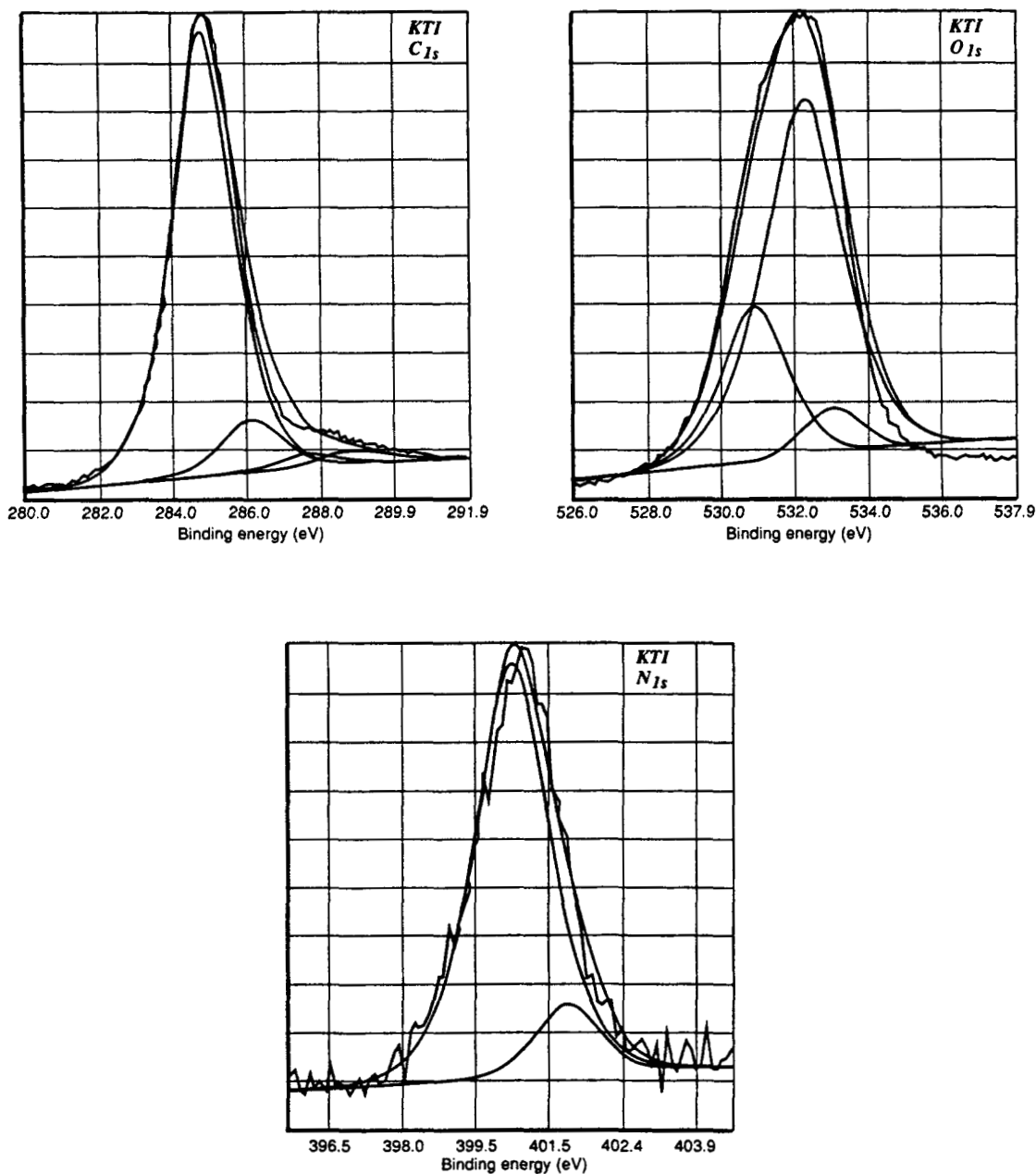
Figure 4 C_{1s}, O_{1s}, and N_{1s} spectra of KTI.

atom. As mentioned in Table I, the O/C ratio of KTI obtained from the total element calculation is as high as 0.562. Now we can calculate the content of oxygen atoms that directly link to carbon atoms from the deconvolution of the C_{1s} peak by $C_2 + C_3 + C_4$ followed by subtraction of nitrogen content (because C_2 includes also the structure of $-C-C-N-$), which is taken from Table I. The value of the O/C ratio for sample KTI obtained in this way is only 0.204, comparable to the O/C value of KPL. This is reasonable, because the fixation of

TiCl$_4$ on the Kevlar fiber surface should not change the amount of oxygen atoms along the macromolecular chains. In other words, the higher O/C ratio calculated from total elements suggests the oxidation of the anchored catalyst when it is exposed to humid air. These oxygen atoms are not linked to carbon atoms and therefore cannot be detected by C_{1s}, but they do exist in this sample and, of course, give a high O/C ratio when calculated from total element calculation. The anchoring of TiCl$_4$ on the Kevlar fiber surface is based on the reaction of the reactive

Table IV   Results of Peak Deconvolution of C_{1s}, O_{1s}, and N_{1s} Spectra of KTI

Atom No.	From Structure	BE_{ref}, eV	BE_{exp}, eV	$P_j/\Sigma\ P_i$
C_1	—C—C—C—	285.0	285.0	0.733
C_2	—C—C—N—, —C—O—	286.3	286.3	0.125
C_3	—CONH—	287.8	287.8	0.068
C_4	—COOH	289.0	289.0	0.074
O_1	—CONH—	531.6		
	—C—O—Ti—	528.6–532.7[20]	531.1	0.254
O_2	O=C—OH	532.8	533.0	0.110
O_3	—C—OH	533.7	—	—
O_4	O=C—OH	534.3	—	—
O_5	—Ti—O	528.6–532.7	532.3	0.637
N_1	—CONH—	401–402	400.3	0.807
N_2	PhNH$_2$	402–403	401.4	0.193

chemical groups such as —COOH and —OH with TiCl$_4$. The anchored Ti is directly linked to the single-bonded oxygen atoms in acid groups or the oxygen atoms in hydroxyl groups. Therefore, the deconvolution of the O_{1s} peak of the catalyst-anchored Kevlar fibers, KTI, should offer more detailed understanding of this process. The comparison of O_{1s} binding energy (BE) data for KPL and KTI shows that the increase in oxygen content after Ti anchoring (see Table I) is mostly associated with the rise of a broad O_{1s} component peak at 532.3 eV (O_5). It is therefore natural to assign this new peak to oxygen linked to Ti. The O_{1s} BE in TiO$_2$ is close to 530.0 ± 0.2 eV.[19] Thus this O_5 component may originate from either TiO$_2$ particles with large differential charging or —Ti—O—C— species on the Kevlar fibers. The replacement of hydrogen atoms in —COOH and —OH by Ti, i.e., the anchoring of TiCl$_4$ on the Kevlar fiber surface, results in the disappearance of O_3 and O_4 and the generation of —Ti—O—C— structure. It is evident that only part of the oxygen atoms in the sample KTI, i.e., O_1 and O_2, are linked to carbon atoms on the Kevlar fibers, and the content of O_5, which results from the oxidation of the anchored catalyst when the fibers

are exposed to air, is 0.637. This is coincident with the conclusion drawn from the C_{1s} peak deconvolution. As to the N_{1s} peak deconvolution, Figures 3 and 4 and Tables III and IV allow that the N_1/N_2 ratio is the same in the spectra of KPL and KTI. This would suggest that —NH$_2$ groups do not interact with titanium tetrachloride. This would be a very surprising conclusion, and the fact that the N-C ratio is smaller in KTI than in KPL indicates a coverage of both —NH— and —NH$_2$ groups by Ti. However, the complete absence of N_{1s} BE shift upon Ti grafting suggests that this does not involve chemical interaction.

Figure 5 shows the C_{1s}, O_{1s}, and N_{1s} spectra of catalytically grafted polyethylene-covered Kevlar fiber (KPOLY). It should be noted that the nitrogen atoms of the Kevlar fibers cannot be detected at all. The signal for nitrogen does not exceed noise, indicating that the polymer coating on the Kevlar fiber hinders XPS from detecting this element. Similarly, the C_{1s} peak of sample KPOLY cannot be deconvoluted into several components, as it did for KOR, KPL, and KTI samples. It involves only C_1 of the structure —C—C—C— (see Fig. 5 and Table V), coming from the polyethylene. Therefore, the oxygen

Table V   Results of Peak Deconvolution of C_{1s} and O_{1s} Spectra of KPOLY

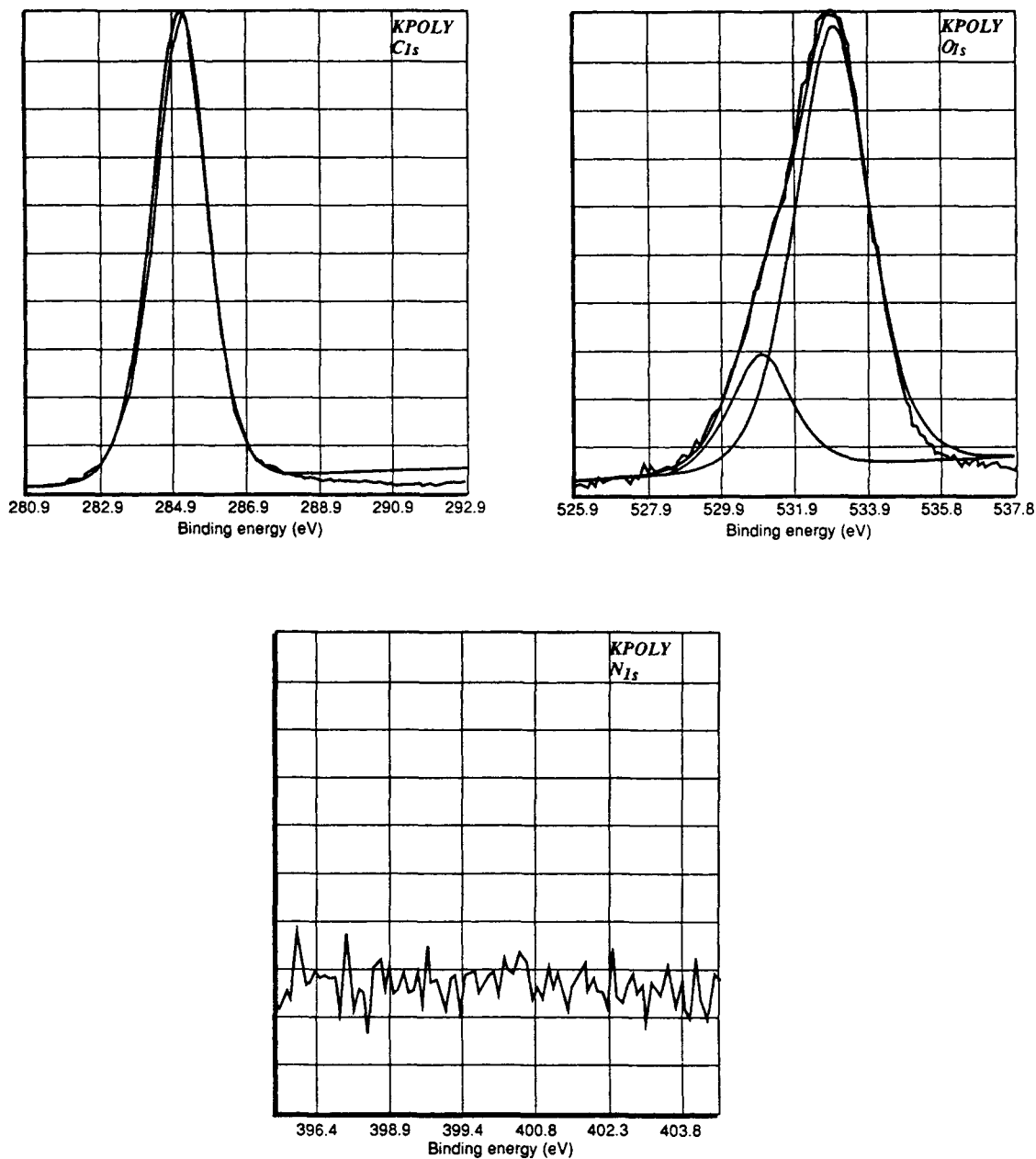| Atom No.	From Structure	BE_{ref}, eV	BE_{exp}, eV	$P_j/\Sigma\ P_i$
C_1	—C—C—C—	285.0	285.1	100
O_1	—Ti—O—	528.6–532.7	531.1	0.199
O_2	—Al—O—	533.3[21]	533.3	0.801

Figure 5 C_{1s}, O_{1s}, and N_{1s} spectra of KPOLY.

signal detected in this sample (see Table I) cannot come from Kevlar fibers. As a tentative explanation for the appearance of two O_{1s} components in the spectrum of KPOLY, it may be suggested that the O_2 component belongs to oxygen linked to aluminum. Indeed, the value reported for O_{1s} in $Al(OH)_3$ is 533.3 eV, which is the BE found for O_2. Aluminum is introduced as $Al(C_2H_5)_3$ during polymerization. The O_1 component would therefore be associated with oxygen linked to titanium.

The structure changes that resulted from oxygen plasma treatment, catalyst fixation, and ethylene polymerization on Kevlar fibers could also be examined by means of IR spectroscopy. However, it was found quite difficult to yield useful IR spectra of fibers by transmission spectroscopy. As an alternative,[22] we employed ATR to investigate the surface structure changes of Kevlar fibers. The spectra of the four samples in the wavenumber range of 1300–1800 cm^{-1} are shown in Figure 6. The amide
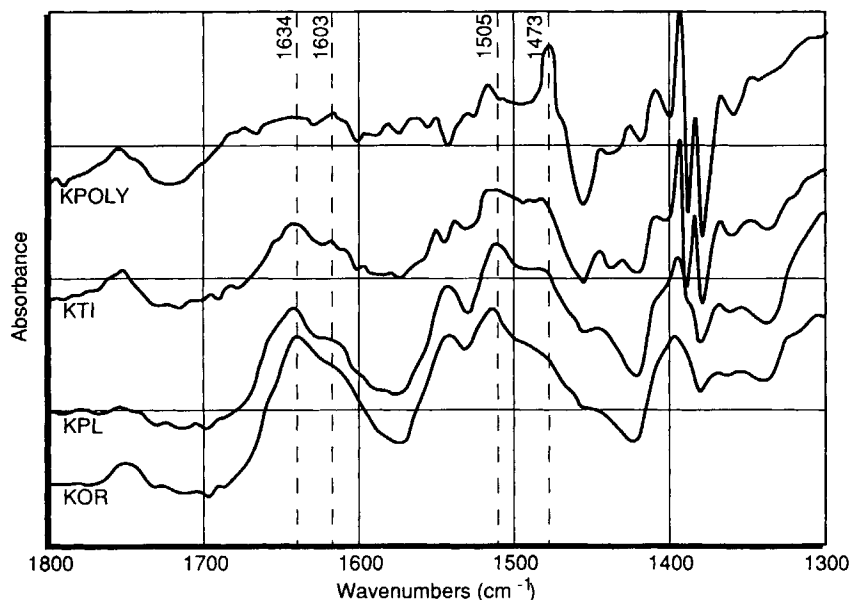
Figure 6 Attenuated total reflection IR spectra of KOR, KPL, KTI, and KPOLY in the region of 1300–1800 cm^{-1}.

band at 1634 cm^{-1} is attributed to the carbonyl stretching vibration $\nu(C=O)$,[23] while other bonds at 1603 and 1505 cm^{-1} are assigned to terminal —NH$_2$ substituent linked to the benzene rings in polyamide.[24] These three bonds are present in the spectra of the original Kevlar fibers (KOR), and they all disappear progressively upon Ti grafting and polyethylene polymerization. The band at 1473 cm^{-1} comes from the scissoring mode of —CH$_2$— in polyethylene,[25] and it appears clearly in the spectrum of KPOLY.

The polyethylene catalytically grafted on Kevlar fibers may form a transition layer between the HDPE polymer matrix and Kevlar fibers in KEG-type composite material. This can be seen from polarized light optical microphotographs (Fig. 7). At room temperature, the grafted and ungrafted Kevlar fibers were embedded in the crystalline polyethylene. With increasing recording temperature, the structure of the grafted polyethylene emerged. When the matrix melted (above 127°C), the transition layer of the grafted polyethylene became clearer (Fig. 7, KEG 131°C). By contrast, the well-defined interface between the ungrafted solid Kevlar filament and the melted polymer matrix is clearly visible (Fig. 7, KEF 131°C). Figure 8 shows the thermal behavior (DSC lines) of the catalytically grafted polymerized Kevlar fibers (KPOLY), the

HDPE composite reinforced by the catalytic grafted Kevlar fibers (KEG), and the composite reinforced by the ungrafted Kevlar fibers (KEF). It could be seen that the polyethylene grafted on Kevlar fibers possesses a higher melting point than the commercial HDPE, and the melting point of the composite reinforced by the grafted Kevlar fibers (KEG) is between the melting points of KPOLY and KEF. This difference may explain the phenomenon observed through the polarized light optical microscope. Similar observations were made when UHMPE fibers were used as a reinforcing agent with polyethylene.[3]

Figures 9 and 10 compare the relative values of tensile modulus, tensile strength, and elongation at break of the composites reinforced by grafted and ungrafted Kevlar fibers, in both directions parallel and transverse to the fibers, where E^* stands for $E/E_{KEF,5\%}$ and $E_{KEF,5\%}$ is 0.902 GPa in the direction parallel to the fibers and 0.248 GPa in the direction transverse to the fibers, respectively. The symbol σ^* stands for $\sigma/\sigma_{KEF,5\%}$, and $\sigma_{KEF,5\%}$ is 28.96 MPa in the direction parallel to the fibers and 8.49 MPa in the direction transverse to the fibers. The symbol ϵ^* stands for $\epsilon/\epsilon_{KEF,5\%}$, and $\epsilon_{KEF,5\%}$ is 3.58% in the direction parallel to the fibers and 11.17% in the direction transverse to the fibers. The improvement by catalytic grafting is very impressive, and the re-
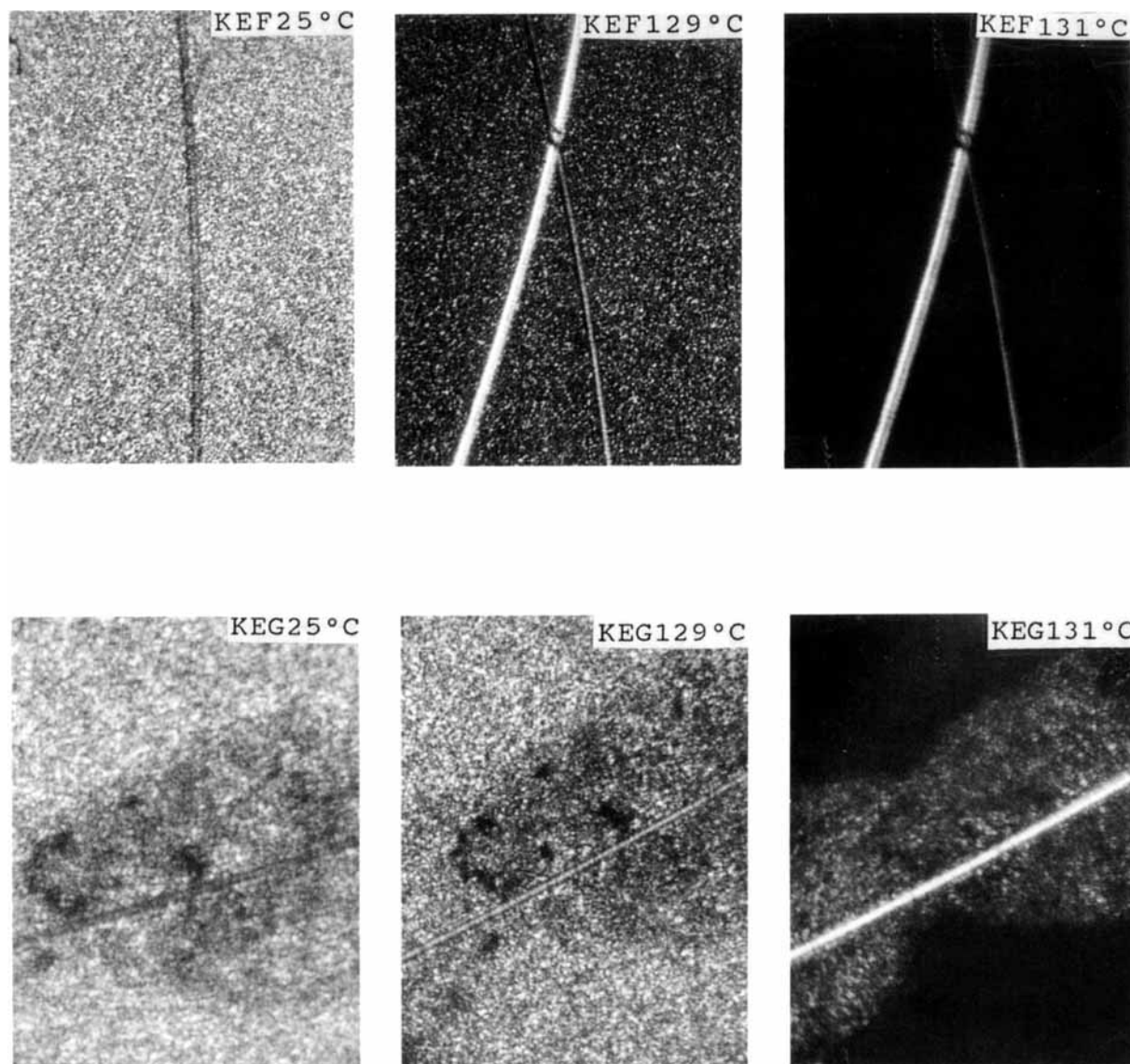
Figure 7 Polarized light optical photographs of the composite films containing a single filament of the catalytic grafted Kevlar fiber (KEG) and the ungrafted Kevlar fiber (KEF) taken at different temperatures.

sult in the direction transverse to fibers (Fig. 10) is of special interest. The increase of tensile strength in this direction of the composites reinforced by grafted Kevlar fibers demonstrates clearly the improvement of interfacial adhesion. The SEM photograms confirm this conclusion. It can be seen from Figures 11 and 12 that after stretching, the ungrafted fibers are pulled out naked (Fig. 11), and the surface of the fibers are smooth, indicating a poor adhesion between the fiber and the polymer matrix. For the

composite reinforced by grafted fibers, however, there is a distinct improvement in the adhesion between the matrix and the reinforcement. The coating of polymer on the fibers is still present after the fibers were pulled out from the matrix. The photograms in the direction transverse to the fibers (Fig. 12) also reveal that the interface of the composite reinforced by grafted Kevlar is rough, and the coating of polymer on the fibers can be observed. In contrast, the interface of the composites reinforced by
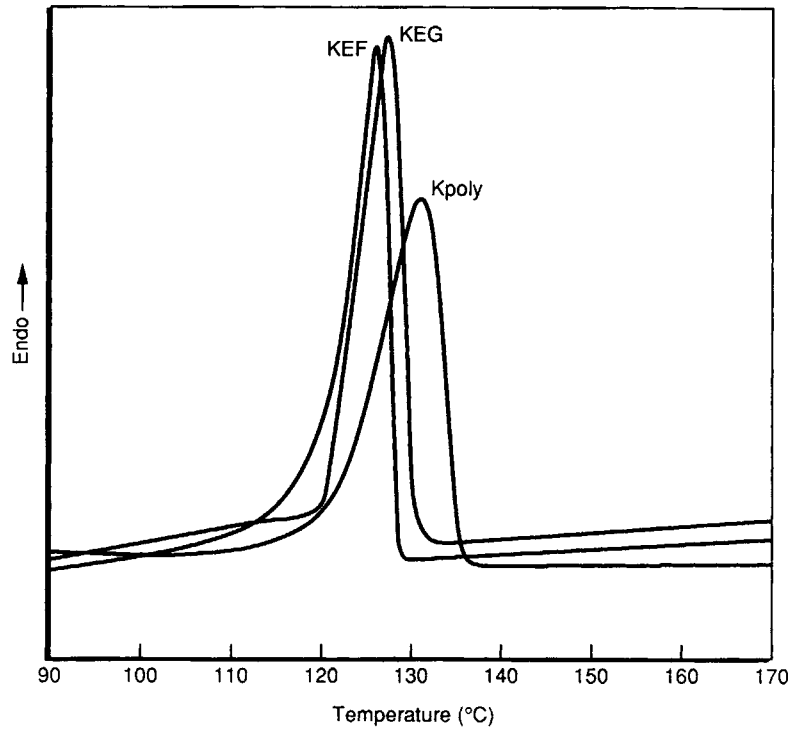
Figure 8   Differential scanning calorimetry curves of the catalytic grafted Kevlar fibers (KPOLY), the HDPE composite reinforced by the catalytic grafted Kevlar fibers (KEG), and the composite reinforced by the ungrafted Kevlar fibers (KEF). Fiber content of KEG and KEF: 5%.
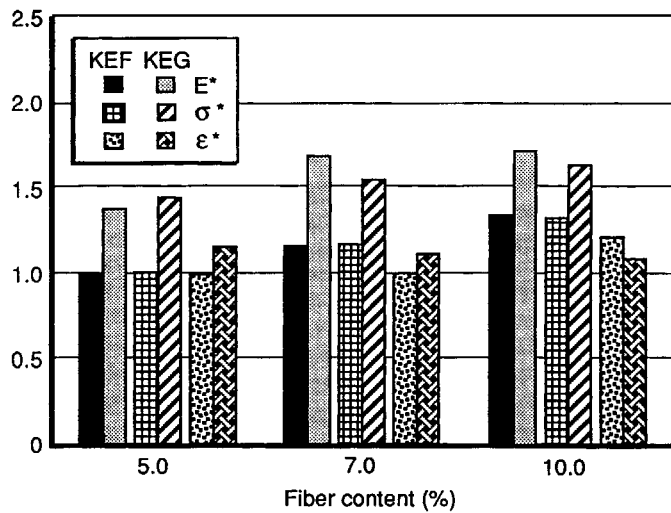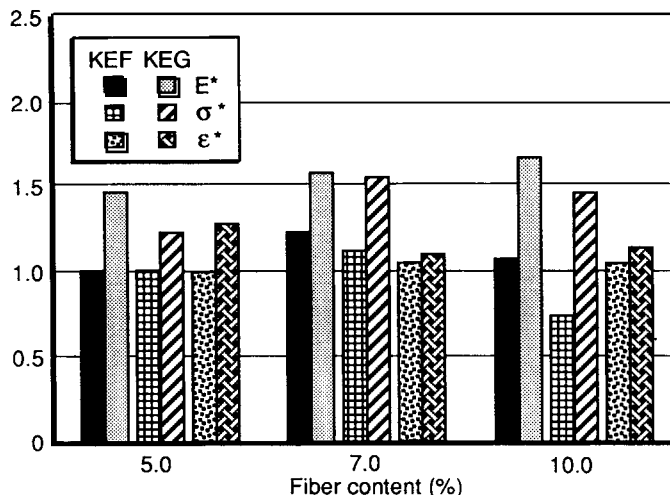

Figure 9   Relative values of modulus, tensile strength, and elongation at break of KEG and KEF types of Kevlar fibers–HDPE composites in the direction parallel to fibers. Here E^* stands for $E/E_{\text{KEF},5\%}$, and $E_{\text{KEF},5\%}$ is 0.902 GPa; σ^* stands for $\sigma/\sigma_{\text{KEF},5\%}$, and $\sigma_{\text{KEF},5\%}$ is 28.96 MPa; and ϵ^* stands for $\epsilon/\epsilon_{\text{KEF},5\%}$, and $\epsilon_{\text{KEF},5\%}$ is 3.58%.

Figure 10   Relative values of modulus, tensile strength, and elongation at break of KEG and KEF types of Kevlar fiber–HDPE composites in the direction transverse to fibers. Here E^* stands for $E/E_{KEF,5\%}$, and $E_{KEF,5\%}$ is 0.248 GPa; σ^* stands for $\sigma/\sigma_{KEF,5\%}$, and $\sigma_{KEF,5\%}$ is 8.49 MPa; and ϵ^* stands for $\epsilon/\epsilon_{KEF,5\%}$, and $\epsilon_{KEF,5\%}$ is 11.17%.

the ungrafted fibers is smooth, indicating a poor interfacial adhesion.

CONCLUSIONS

Oxygen plasma treatment modifies the surface structure of Kevlar fibers effectively. The reactive sites, namely, —COOH, —OH, and possibly —NH₂ could be used to anchor catalysts. This was then followed by Ziegler–Natta polymerization of ethylene on the Kevlar fibers. Scanning electron microscopy, XPS, and ATR offered a detailed un-

derstanding of these procedures. The grafted polyethylene acts as a transition layer between the polymer matrix and the reinforcement and improves the interfacial adhesion, therefore enhancing the mechanical properties significantly, in both directions either parallel or transverse to the fibers.

It is expected that the principle of this technique will be applied to numerous other systems. The catalysts that can be anchored on the fiber surface are not limited to Ziegler–Natta catalysts only. Similar application of polymer synthesis onto fiber surfaces may be suggested for radical polymerization, ionic as well as condensation polymerization.
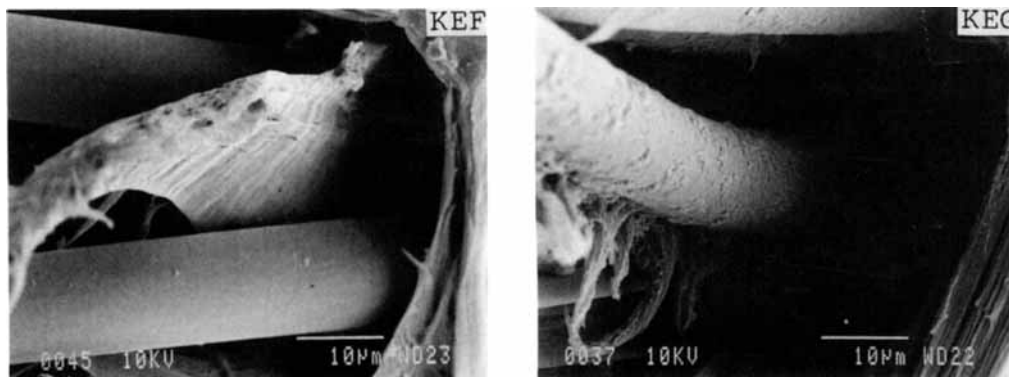

Figure 11   Scanning electron micrographs of KEG and KEF types of Kevlar fiber–HDPE composites in the direction parallel to fibers after stretching. (×2000)
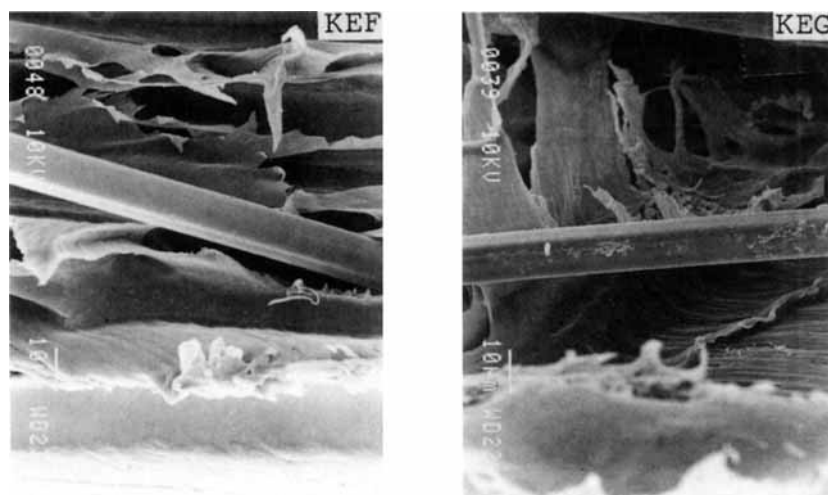
Figure 12   Scanning electron micrographs of KEG and KEF types of Kevlar fiber–HDPE composites in the direction transverse to fibers after stretching. (×1000)

REFERENCES

1. P. Frissel, in *Encyclopedia of Polymer Science & Technology*, vol. 6, Wiley, New York, 1967, p. 740.
2. Q. Wang, S. Kaliaguine, and A. Ait-Kadi, *J. Appl. Polym. Sci.*, **44**, 1107–1119 (1992).
3. Q. Wang, A. Ait-Kadi, and S. Kaliaguine, *J. Appl. Polym. Sci.*, **45**, 1023 (1992).
4. Q. Wang, A. Ait-Kadi, and S. Kaliaguine, *Polym. Composites*, to appear.
5. D. J. Vanghan, *Polym. Eng. Sci.*, **18**, 167 (1978).
6. D. B. Eagles, B. F. Brumentritt, and S. L. Cooper, *J. Appl. Polym. Sci.*, **20**, 435 (1976).
7. M. Breznick, J. Banbaji, H. Cuttmann, and G. Marom, *Polym. Comm.*, **28**, 55 (1987).
8. M. Tagayanagi, T. Kajirama, and T. Katayose, *J. Appl. Polym. Sci.*, **27**, 3903 (1982).
9. A. G. Andreopoulos, *J. Appl. Polym. Sci.*, **38**, 1053 (1989).
10. Z. Yu, A. Ait-Kadi, and J. Brisson, *Polym. Eng. Sci.*, **31**, 1228 (1991).
11. R. J. Morgan and C. O. Pruneda, *Polymer*, **28**, 340 (1987).
12. T. S. Keller, A. S. Hoffman, B. D. Ratner, and B. J. McElroy, *Physicochemical Aspects of Polymer Surfaces*, K. L. Mittal (Ed.), Plenum, New York, 1983.
13. R. Borade, A. Sayari, A. Adnot, and S. Kaliaguine, *J. Phys. Chem.*, **94**, 5989 (1990).
14. S. L. Kaplan and P. W. Rose, *Int. J. Adhesion Adhesive*, **11**, 109 (1991).
15. G. Grespi, in F. Mark and D. F. Othmer (Eds.), *Encyclopedia of Chemical Technology*, 3rd ed., Vol. 16, Wiley, New York, p. 459.
16. U. Zucchini and G. Cecchini, *Adv. Polym. Sci.*, **51**, 107 (1983).
17. A. Dilks, in *Developments in Polymer Characterization*, Vol. 2, J. V. Dawkins (Ed.), Applied Science Publishers, 1981, p. 145.
18. D. T. Clark, B. J. Cromarty, and A. Dilks, *J. Polym. Sci. Polym. Chem. Ed.*, **16**, 3173 (1978).
19. D. T. Clark and H. R. Thomas, *J. Polym. Sci. Polym. Chem. Ed.*, **16**, 791 (1978).
20. S. M. Mukhopadhyay and S. H. Carofalini, *J. Non-Cryst. Solids*, **126**, 202 (1990).
21. C. D. Wagner, W. M. Giggs, L. E. Davis, J. F. Moulder, and G. E. Muilenberg, *Handbook of X-Ray Photoelectron Spectroscopy*, Perkin-Elmer Co., Eden Prairie, 1978, p. 42.
22. H. W. Siesler and K. Holland-Miritz, *Infrared and Raman Spectroscopy of Polymers*, Marcel Dekker, New York, 1980, p. 128.
23. H. W. Siesler and K. Holland-Miritz, *Infrared and Raman Spectroscopy of Polymers*, Marcel Dekker, New York, 1980, p. 302.
24. D. Dolphin and A. Wick, *Tabulation of Infrared Spectral Data*, Wiley, New York, 1977, p. 7.
25. C. N. R. Rao, *Chemical Application of Infrared Spectroscopy*, Academic Press, New York, 1963, p. 131.